Proc. 5th Int. Symp. Turbulence and Shear Flow Phenomena
Munich, Germany, August 27-29, pp. 1167-1172

Systematic Analysis of High Schmidt Number Turbulent Mass Transfer Across Clean, Contaminated and Solid Interfaces

Yosuke Hasegawa & Nobuhide Kasagi
Department of Mechanical Engineering,
The University of Tokyo
Hongo 7-3-1, Bunkyo-ku, Tokyo, 113-8656, Japan
hasegawa@thtlab.t.u-tokyo.ac.jp, kasagi@thtlab.t.u-tokyo.ac.jp

ABSTRACT

A series of numerical simulation is carried out of high Schmidt number turbulent mass transfer across interfaces of different dynamical conditions, i.e., a clean or contaminated free surface and also a solid surface. With increasing the Marangoni number representing the surface tension effect, low-frequency fluctuations of surface divergence, which play a critical role in the interfacial mass transfer, are drastically decreased. Various statistics of the turbulent concentration fluctuation reveal that the transport mechanism at a contaminated interface becomes dynamically equivalent to that at a solid surface beyond a critical Marangoni number. Consequently, the interfacial gas transfer rate falls down to that on a solid surface, so that the Schmidt number exponent switches from –0.5 to –0.7. Based on a one-dimensional advection-diffusion equation, a criterion for the transition of the turbulent mass transfer mode is discussed.

INTRODUCTION

It is well known that surface contamination drastically retards interfacial mass transfer. Up to now, numerous studies of gas transfer across clean and contaminated air-water interfaces have been carried out in wind-wave facilities and stirred vessels, e.g., Jähne et al. (1987) and Asher and Pankow (1986). In these studies, a common trend has been observed. Specifically, the gas transfer rate K_w increases only slowly with wind speed below a critical wind velocity, while it suddenly increases beyond the critical wind velocity. It was also confirmed that the Schmidt number dependence of K_w switches from $K_w \propto Sc^{-0.7}$ to $K_w \propto Sc^{-0.5}$ above the critical wind velocity (Jähne et al., 1987). Since the analogy between the mass transfer and momentum/heat transfer is often used in predicting the mass transfer rate, the Schmidt number dependency of K_w is crucial in practical applications.

In a previous study (Hasegawa and Kasagi, 2005), it was demonstrated that this transition can be reproduced in numerical simulation by changing the Marangoni number, which represents the degree of surface elasticity arising from surface-active agents. It is worth noting that the concentration field near clean and slightly contaminated interfaces quickly responds to the interface-normal velocity fluctuation even at high Schmidt numbers. Near a highly contaminated interface, however, high-frequency concentration fluctuations are strongly damped. This drastic change is analogous to a difference between free and solid surfaces in terms of interfacial mass transfer (Hasegawa and Kasagi, 2007). Namely, lower-velocity fluctuations govern the mass transfer across a solid surface, while a wide range of frequencies plays an important role at a free surface.

Although the previous studies suggest the transition of the turbulent transfer mode beyond a critical Marangoni number, the transition mechanism and the effects of surface elasticity on statistics of the concentration field have not been reported in detailed so far.

In the present paper, we systematically conduct numerical simulation of high Schmidt number mass transfer across clean, contaminated and solid interfaces in order to understand how an interfacial dynamical condition influences the interfacial mass transfer. We will proceed as follows. First, we show the fundamental statistics inside the concentration boundary layer. Then, we study the response of the concentration field to the interface-normal velocity fluctuation via frequency analyses. Finally, we discuss a critical parameter which governs the transition of the turbulent mass transfer mode at a contaminated interface.

NUMERICAL PROCEDURES

Numerical Conditions

We consider a counter-current air-water flow driven by a constant pressure gradient. The flow geometry and the coordinate system are shown in Fig. 1, where x, y and z are the streamwise, interface-normal and spanwise directions, respectively. Thourghout the present paper, the subsripts of a and w represent values in the air and water phases, respectively. A value with asterisk is a dimensional value.

The governing equations are the incomperessible Navier-Stokes, continuity and scalar transport equations:

$$\frac{\partial u_i}{\partial t} + \frac{\partial \left(u_j u_i \right)}{\partial x_j} = -\frac{\partial p}{\partial x_i} + \frac{1}{Re_\tau} \frac{\partial^2 u_i}{\partial x_j \partial x_j} \tag{1}$$

$$\frac{\partial u_i}{\partial x_i} = 0 \tag{2}$$

$$\frac{\partial c}{\partial t} + \frac{\partial \left(u_j c \right)}{\partial x_j} = \frac{1}{Sc \cdot Re_\tau} \frac{\partial^2 c}{\partial x_j \partial x_j} \tag{3}$$

Proc. 5th Int. Symp. Turbulence and Shear Flow Phenomena
Munich, Germany, August 27-29, pp. 1167-1172

Here, all the variables are non-dimensionalized by the interfacial friction velocity u^*_τ and the depth δ^*. The concentration c is normalized by the concentration difference ΔC between the interface and the bottom of the compuational domain. The Reynolds numbers based on u^*_τ and δ^* are $Re_{\tau w} = Re_{\tau a} = 150$, which approximately corresponds to a countercurrent air-water flow with u^*_a = 2.2 m/s and u^*_w = 0.054 m/s at two outer boundaries of δ^* = 4cm. The density ratio of water and air is $\rho^*_w / \rho^*_a = 841$. The Schmidt number in the water phase is set to be Sc_w = 1.0 and 100. A periodic boundary condition is employed for the horizontal directions, while a free-slip condition for outer boundaries so as to minimize their effects. In addition to Eqs. (1-3), a transport equation of a surfactant concentration γ is solved at the interface.

$$\frac{\partial \gamma}{\partial t} + \frac{\partial (u_j \gamma)}{\partial x_j} = \frac{1}{Sc_\gamma \cdot Re_\tau} \frac{\partial^2 \gamma}{\partial x_j \partial x_j} \quad (j = 1 \text{ and } 3) \qquad (4)$$

The surfactant concentration and the velocity field are coupled through an interfacial boundary condition described in the following subsection. Direct numerical simulation (DNS) is applied to the velocity field and the concentration field at the low Schmidt number of 1.0 by using a pseudo-spectral method. For the high Schmidt number of 100, a hybrid DNS/LES scheme is employed.

Hybrid DNS/LES Method

Since the thickness δ_c of the concentration boundary layer decreases with the Schmidt number as $\delta_c \propto Sc^{-1/2}$ and $\delta_c \propto Sc^{-1/3}$ for free and solid interfaces, respectively, we apply a hybrid DNS/LES method, in which DNS with high-resolution grids is employed within the thin concentration boundary layer, while large-eddy simulation (LES) with coarse grids in the outer layer.

The computational domain in the water phase is divided into three regions, i.e., a DNS region ($0 < y^+ < 11.3$), a switching region ($11.3 < y^+ < 21.5$) and a LES region ($y^+ > 21.5$). Depth of the DNS region is determined so that 95% of a concentration change occurs in this region. The details of the numerical scheme and its verification can be found in Hasegawa and Kasagi (2007). Number of modes employed the present calculations are listed in Table 1.

Interfacial Boundary Conditions

Since we focus on the effects of surface elasticity on high Schmidt number mass transfer, the interfacial deformation is neglected in order to avoid additional complexity. The resultant boundary conditions at an air-water interface are the continuity of the horizontal velocity components and the force balance between the shear stresses exerted by the air and water flows, and the surface tension.

$$u_{wj} = \sqrt{\frac{\rho_w}{\rho_a}} u_{aj} \qquad (5)$$

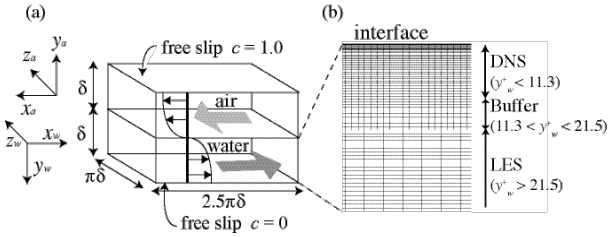

Figure 1: a) Computational domain, b) grid system in hybbrid DNS/LES

Table 1: Number of modes and grids

		Region	k_x, k_y or N_y, k_z	Δx_L^+	Δy_L^+	Δz_L^+
Velocity	DNS	$0 < y_L^+ < 150$	64, 128, 64	18.4	0.002 ~ 0.38	7.2
Scalar: Hybrid DNS/LES	DNS	$0 < y_L^+ < 11.3$	192, 35, 192	6.1	0.01 ~ 0.62	2.4
	Buffer	$11.3 < y_L^+ < 21.6$	192, 13, 192	6.1	0.66 ~ 0.85	2.4
	LES	$21.6 < y_L^+ < 150$	64, 144, 64	18.4	0.86 ~ 1.23	7.2

Table 2: Computational conditions

	Ma	*We*
Clean	0	9.0×10^{-3}
Case 1	1.0×10^{-3}	9.0×10^{-3}
Case 2	1.0×10^{-2}	9.0×10^{-3}
Case 3	1.0×10^{-1}	9.0×10^{-3}
Solid	-	-

$$\frac{1}{Re_{\tau w}} \frac{\partial u_{wj}}{\partial y_w} = \frac{1}{Re_{\tau a}} \frac{\partial u_{aj}}{\partial y_a} + \frac{Ma}{We} \frac{\partial \gamma}{\partial x_j} \qquad (6)$$

Here, j is 1 or 3. The second term on the right-hand-side of Eq. (6) represents the surface elasticity. The Weber number *We* and the Marangoni number *Ma* are defined as $We = \rho_w u_{\tau w}^2 \delta / \sigma_0$ and $Ma = -(\gamma_0 / \sigma_0)(d\sigma / d\gamma)_0$, respectively. The subscript 0 represents evaluation at equilibrium and σ is the surface tension. In the present study, *Ma* is changed systematically as *Ma* = 0 (clean), 10^{-3} (Case 1), 10^{-2} (Case 2), 10^{-1} (Case 3), while *We* is kept constant *We* = 9.0×10^{-3}. Hereafter, we will focus on only the water phase and omit the subscript of *w*. In addition to clean and contaminated interfaces, turbulent mass transfer across a solid surface is also considered as a extreme case by replacing a free surface with a no-slip boundary. All the cases considered in the present study are listed in Table 2.

For the concentration field, a constant concentration boundary condition c = 1 is imposed at the interface, while c = 0 at the bottom.

VELOCITY FIELD

Velocity fluctuation

Velocity fluctuations near clean, contaminated and solid interfaces are plotted in Fig. 2. With increasing the Marangoni number, the normal velocity fluctuation is drastically damped, while the streamwise and spanwise velocity fluctuations are almost unchanged. This indicates that the highly contaminated interface is essentially different from a solid wall. The thickness of the region in which

Proc. 5th Int. Symp. Turbulence and Shear Flow Phenomena
Munich, Germany, August 27-29, pp. 1167-1172

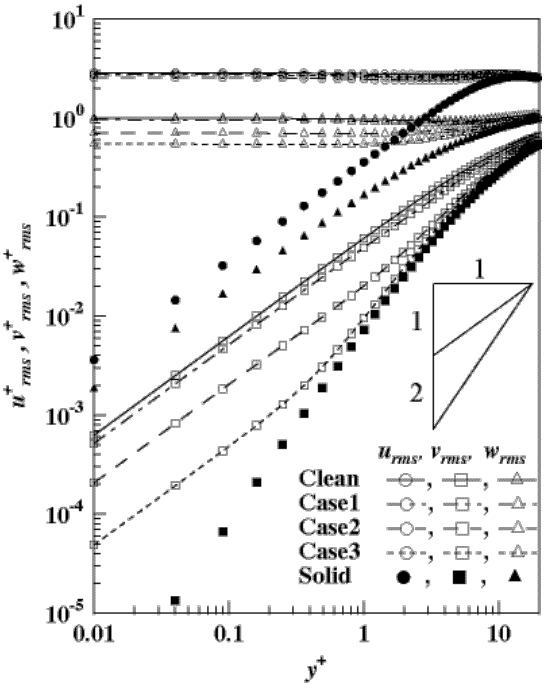

Figure 2: Velocity fluctuation near interface

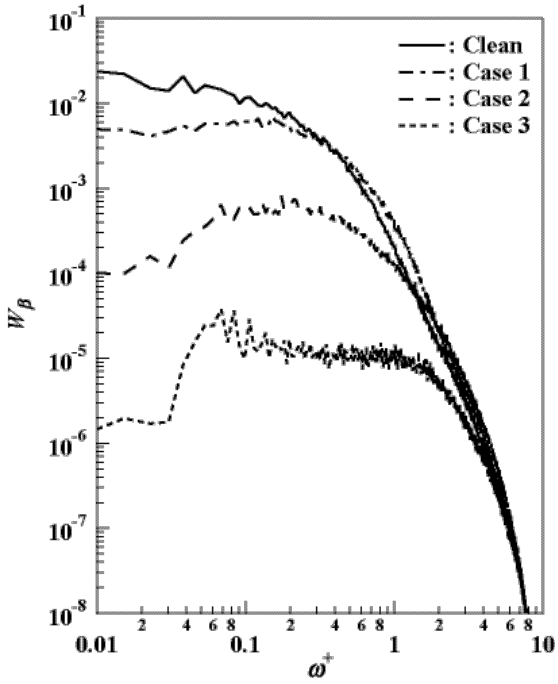

Fig. 3 frequency spectrum of surface divergence

$v \propto y$ is decreased with the Marangoni number. As a result, the normal velocity fluctuation in Case 3 converges to the data near the solid surface in the region of $y^+ > 1$.

As discussed in McCready and Hanratty (1984), limiting behavior of the normal velocity fluctuation toward the interface plays a critical role in the interfacial mass transfer. In the case of a flat interface considered here, the normal velocity fluctuation is approximated by the first term in a Taylor series as:

$$v(y,t) \simeq -\beta(t)\, y \tag{7}$$

Here, β is called the surface divergence defined as $\beta = (-\partial v / \partial y)_{y=0}$. In Fig. 3, the frequency spectrum of β is plotted. Low-frequency fluctuations are drastically damped due to surface contamination. This is the primal reason for the change of a turbulent transfer mode discussed below.

FUNDAMENTAL CONCENTRATION STATISTICS

Mean Concentration

The mean concentration profiles near the clean, contaminated and solid interfaces at *Sc* = 100 are presented in Fig. 4. The abscissa is the distance from the interface in the shear unit. The ordinate is the mean concentration relative to the interfacial concentration non-dimensionalized by the friction concentration. A distinct difference between the mean profiles near the clean and solid interfaces can be found. It is also observed that with increasing the Marangoni number, the mean concentration approaches to that near the solid interface.

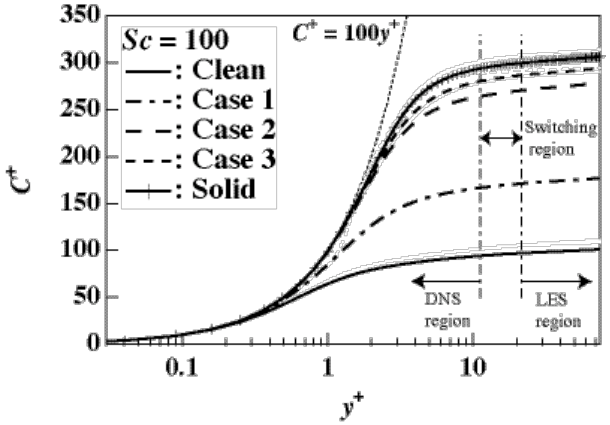

Figure 4: Mean concentration profile

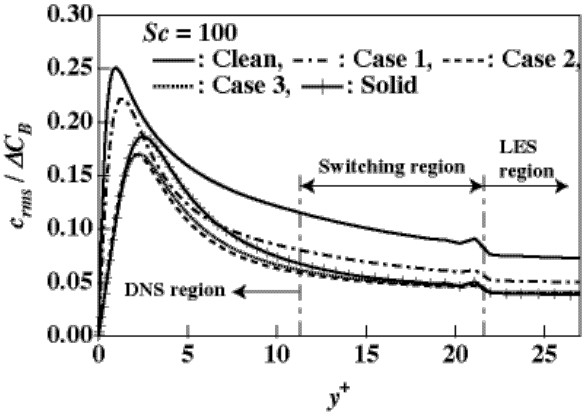

Figure 5: Concentration fluctuation

Proc. 5th Int. Symp. Turbulence and Shear Flow Phenomena
Munich, Germany, August 27-29, pp. 1167-1172

Concentration Fluctuation

The concentration fluctuation c_{rms} at Sc = 100, which is normalized by the difference ΔC_B between the interfacial and bulk concentrations, is shown in Fig. 5. With increasing the Marangoni number, the peak value is decreased and the peak location y^+_p moves futher from the interface, i.e., y^+_p = 1.0, 1.2 and 2.2 for clean and contaminated interfaces (Cases 1 and 2), respectively. Although the profile of concentration fluctuation coverges at highly contaminated interfaces (Cases 2 and 3), it slightly deviates from that near a solid surface. This may be attributed to the large tangential velocity fluctuations at a contamintaed interface (see, Fig. 2).

TRANSITION OF TRANSPORT MECHANISM

Gas Transfer Rate

The gas transfer rates at Sc = 1.0 and 100 are plotted in Fig. 6. With increasing the Marangoni number, the gas transfer rate is decreased drastically and eventually converges to the value on a solid surface. Surface contamination has a profound effect at the high Schmidt number, since the most resistance to mass transfer lies in a thinner layer beneath the interface. Specifically, the gas transfer rate is decreased by 60 % at Sc = 100, while only 25% at Sc = 1.0. Experimental data at clean and highly contaminated interfaces by Jähne et al. (1987) are also plotted in Fig. 6. Good agreement between the present results and the experimental data is confirmed. Although only two data points are available, it is observed that the Schmidt number exponent changes from -0.5 at clean and slightly contaminated interfaces to -0.7 at a highly contaminated interface.

Eddy Diffusivity

The change of the turbulent transfer mode clearly appears in the limiting behavior of an eddy diffusivity E_d shown in Fig. 7. Considering the limiting behavior of velocity and concentration fluctuations, the eddy diffusivity varies as $E_d \propto y^2$ and $E_d \propto y^3$ close to free and solid surfaces, respectively. In the case of clean and slightly contaminated interfaces (Case 1), E_d^+ is proportional to y^{+2}. With increasing the Marangoni number, however, the region in which $E_d \propto y^2$ is decreases and lies in the molecular-diffusive sublayer, where the turbulent transport is not significant. Eventually, E_d converges to the data near a solid surface. These results are consistent with the change of the Schmidt number exponent of K shown in Fig. 6.

Correlation between Velocity and Concentration Fields

The correlation coefficient between concentration and normal velocity fluctuations R_{cv} are plotted in Fig. 8. R_{cv} is drastically decreases with increasing the Marangoni number and eventually, converges to the data near a solid surface. Hasegawa and Kasagi (2007) observed that the concentration field close to a solid surface becomes less sensitive to the normal velocity fluctuation at high Schmidt numbers. The present results indicate a highly contaminated interface is analogous to a solid surface in terms of the response of the concentration boundary layer to the normal velocity fluctuation.

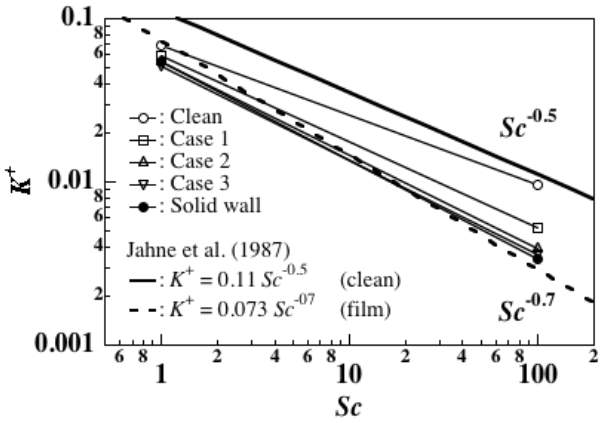

Figure 6: Gas transfer rates

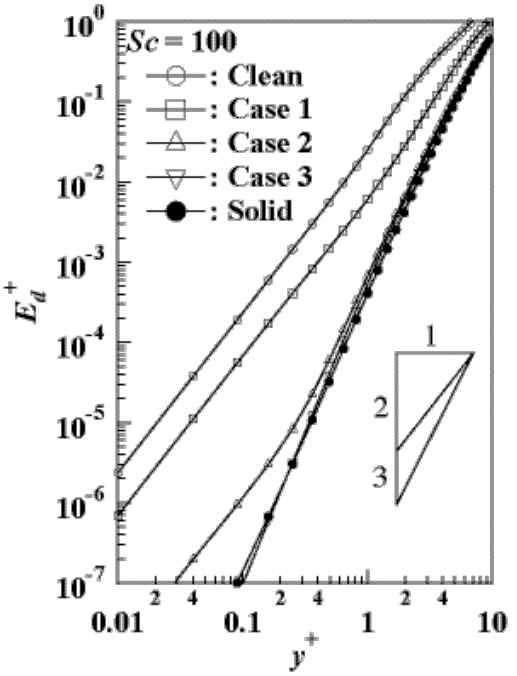

Figure 7: Limiting behavior of eddy diffusivity

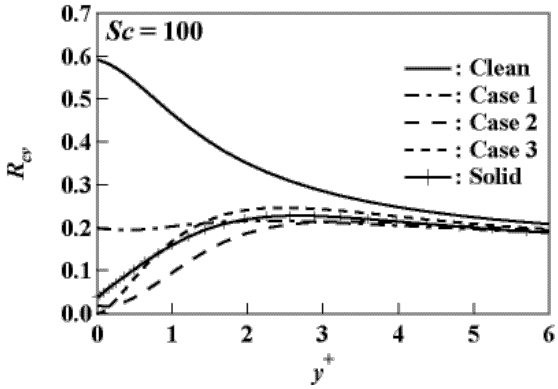

Figure 8: Correlation coefficient R_{cv}

Proc. 5th Int. Symp. Turbulence and Shear Flow Phenomena
Munich, Germany, August 27-29, pp. 1167-1172

FREQUENCY ANALYSES

Frequency Spectrum of Interfacial Mass Flux

The frequency spectrum W_q/Q^2 of interfacial mass flux q are shown in Fig. 9. According to the analysis of a one-dimensional advection-diffusion equation by McCready and Hanratty (1984), the following relationship is obtained:

$$\frac{W_q}{Q^2} = \frac{W_\beta}{\omega^2} \tag{8}$$

Here, W_β is a frequency spectrum of surface divergence β and Q is the mean mass flux. At high frequencies, the present results agree fairly well with Eq. (8). On the other hand, at low frequencies, the concentration fluctuation deteriorates with increasing the Marangoni number, and eventually converges to the data at a solid surface. The damping of low-frequency concentration fluctuations explains the decrease of the peak value of $c_{\rm rms}$ near contaminated interfaces (see, Fig. 3).

The above results indicate that a frequency range in which Eq. (8) holds gets higher and narrower with increasing the Marangoni number, while lower-frequency concentration fluctuations behave more like those near a solid surface.

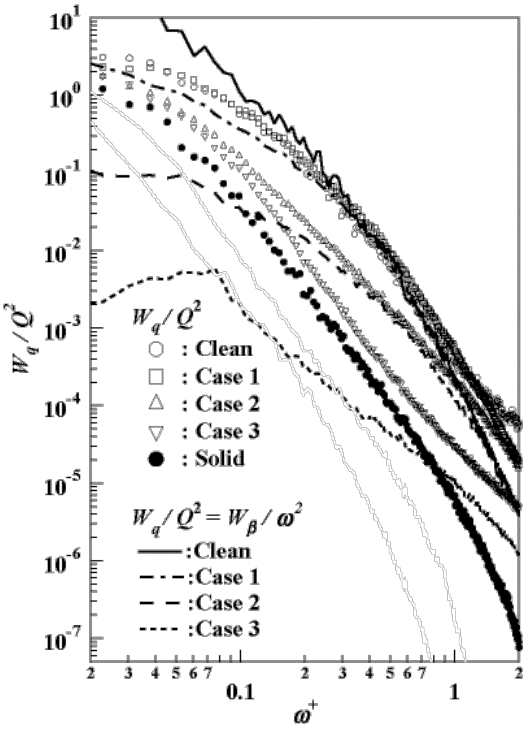

Figure 9: Frequency spectra of interfacial mass flux.

Contribution to Turbulent Mass Transfer at Different Frequencies

The damping of low-frequency concentration fluctuations influences the transport mechanism close to a contaminated interface. Frequency cospectra W_{cv} of $\overline{c'v'}$ at y^+ = 1.1 near clean and highly contaminated interfaces (Case 2) are shown in Figs. 10 a) and b), respectively. Here, W_{cv} is defined as:

$$\overline{c'v'} = \int_{\omega=0}^{\infty} W_{cv}(\omega)\, d\omega \tag{9}$$

In the case of a clean interface, the profile is almost independent of the Schmidt number. This indicates that the frequency range which contributes to mass transfer is alomst the same. On the other hand, near a highly contaminated interface (see, Fig. 10 b)), it is observed that the mass transfer at the high Schmidt number is controled by lower frequencies. This trend is quite similar to results near a solid surface (Hasegawa and Kasagi, 2007).

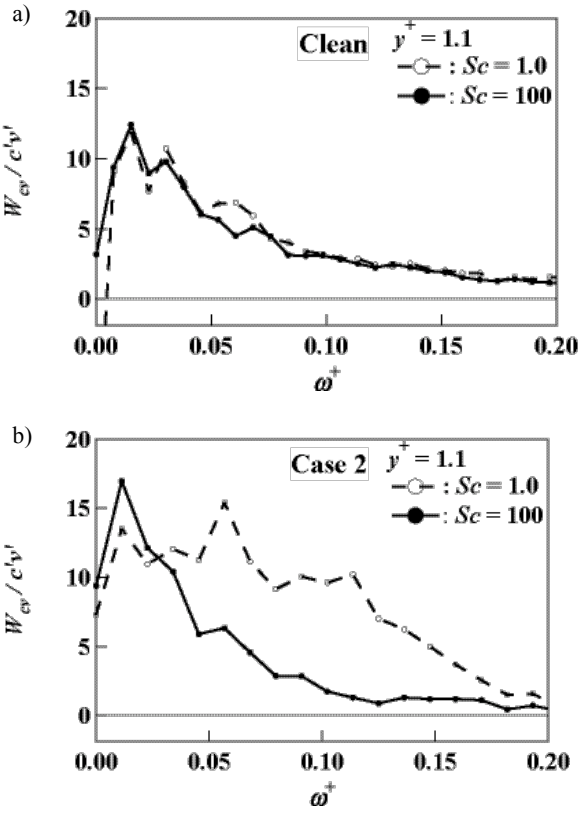

Figure 10: Frequency cospectra a): Clean, b) Case2

DISCUSSIONS

The present results indicate that the characteristics of the concentration field and the transport mechanism near a contaminated interface become equivalent to those near a solid surface beyond a critical Marangoni number. In order to consider a critical parameter for the transition of the turbulent mass transfer mode, the following one-dimensional advection-diffusion equation is revisited.

$$\frac{\partial c}{\partial t} + v\frac{\partial c}{\partial t} = \frac{1}{Sc}\frac{\partial^2 c}{\partial y^2} \tag{10}$$

Here, all variables are normalized by shear unites. Considering a thin concentration boundary layer, v is approximated by $-\beta(t)y$. Hasegawa and Kasagi (2005) considered a single sinusoidal wave, i.e.,

$\beta(t) = \sqrt{2}\beta_0 \cos(\omega_0 t)$. By introducing a new coordinate $Y = \sqrt{Sc\omega_0}\, y$ and a time-scale $T = \omega_0 t$, the Schmidt number disappears from Eq. (10) and the only remaining parameter is β_0 / ω_0 as follows:

$$\frac{\partial c}{\partial T} - \sqrt{2}\frac{\beta_0}{\omega_0}\cos(T)\frac{\partial c}{\partial Y} = \frac{\partial^2 c}{\partial Y^2} \qquad (9)$$

Hasegawa and Kasagi (2005) showed that β contributes to mass transfer only when $\beta_0 / \omega_0 >> 1$.

Similarly, in the case of a turbulent air-water interface, in order for β to contribute to the mass transfer, a frequency spectrum of β should lie below a critical frequency, i.e., $\omega << \beta_{rms}$. The ratio of energy contained in the frequency range of $\omega < \beta_{rms}$ to total energy can be calculated from the frequency spectra in Fig. 3. They are listed in Table 3. Since low-frequency fluctuations are drastically damped at a contaminated interface (see, Fig. 3), the effective surface divergence rapidly decreases with increasing the Marangoni number. Especially, in the highly contaminated interfaces (Cases 2 and 3), the ratio is almost zero, which indicates that most surface divergence does not contribute to the interfacial mass transfer. This should be a primal reason why the turbulent mass transfer mechanism near the highly contaminated interface transits to that near a solid surface.

Table 3: Ratio of effective surface divergence

	Ratio
Clean	74 %
Case 1	18 %
Case 2	2.5 %
Case 3	0.6 %

CONCLUSIONS

Numerical simulation of high Schmidt number turbulent mass transfer across clean, contaminated and solid interfaces was systematically carried out in order to clarify the effects of an interfacial dynamical condition on the interfacial mass transfer. Due to the surface elasticity, the interfacial normal velocity fluctuation at low frequencies is rapidly decreased. This causes drastic changes in the turbulent transport mechanism near a contaminated interface.

Specifically, the region where the eddy diffusivity E_d varies as $E_d \propto y^2$ becomes narrower with increasing the Marangoni number, and eventually the profile converges to that near a solid surface, i.e., $E_d \propto y^3$. As a result, the Schmidt number exponent of the gas transfer rate switches from –0.5 to –0.7. It was also observed that only low-frequency velocity fluctuations penetrate the concentration boundary layer and contribute to the mass transfer near a contaminated interface. All of these results indicate that the transport mechanism at a highly contaminated interface is dynamically equivalent to that at a solid surface beyond a critical Marangoni number.

In the interfacial mass transfer, the surface divergence, which represents the intensity of the interface-normal velocity fluctuations close to an interface, plays a important role. Since the fluctuating surface divergence contributes to the interfacial mass transfer only when its frequency is sufficiently smaller than its magnitude, i.e., $\omega << \beta_{rms}$, a frequency spectrum of the surface divergence is crucial information for predicting the transition of the turbulent mass transfer mode. The present results showed that the ratio of energy contained in the frequency range of $\omega < \beta_{rms}$ to the total energy can be used as a criterion for the transition. Since low-frequency fluctuations of the surface divergence are drastically damped at a contaminated interface, the effective surface divergence, which contributes to the mass transfer, almost vanishes beyond a critical Marangoni number. This should be a main reason for the transition of the turbulent transport mode at a contaminated interface.

ACKNOWLEDGMENT

The present work was supported through the 21st Century COE Program, “Mechanical Systems Innovation.” by the ministry of Education, Culture, Sports, Science and Technology.

REFERENCES

Asher, W. and Pankow, J. F., 1986, "The interaction of mechanically generated turbulence and interfacial films with a liquid phase controlled gas/liquid transport process", Tellus, Vol. 38B, pp. 305-318.

Jähne, B., Männich, K. O., Bösinger, R., Dutzi, A. Huber, W., and Libner, P., 1987, "On the Parameters Influencing Air-Water Gas Exchange", Journal of Geophysical Research, Vol. 92, No. C2, pp. 1937-1949.

Hasegawa, Y., and Kasagi, N., 2005, "Turbulent Mass Transfer Mechanism across a Contaminated Air-Water Interface", Proceedings, 4th International Symposium on Turbulent Shear Flow Phenomena, pp. 971-976.

Hasegawa, Y., and Kasagi, N., 2007, "Effect of Interfacial Boundary Condition on Turbulent Mass Transfer at High Schmidt Numbers", International Journal of Heat and Fluid Flow, accepted.

Lombardi, P., De Angelis V. and Banerjee, S., 1996, "Direct numerical simulation of near-interface turbulence in coupled gas-liquid flow", Physics of Fluids, Vol. 8, pp. 1643-1665.

McCready, M. J. and Hanratty, T. J., 1984, "Concentration Fluctuations close to a Gas-Liquid Interface", A.I.Ch.E. Journal, Vol. 30, No. 5, pp. 816-817.

Shaw, D. A. and Hanratty, T. J., 1977, "Influence of Schmidt Number on the Fluctuations of Turbulent Mass Transfer to a Wall", A.I.Ch.E. Journal, Vol. 23, No. 2, pp.160-169.